Chapter 3

POREWATER REDOX GEOCHEMISTRY BEFORE AND AFTER EXPOSURE AND RE-SUBMERGENCE OF SEDIMENT AT A RESERVOIR SHORELINE

Richard A. Wildman, Jr., Nathan C. Chan,

Nathan F. Dalleska, Mark Anderson, and Janet G. Hering

(submitted to *Limnology and Oceanography*)

Acknowledgements

The authors thank K.M. Campbell, M.A. Ferguson, A.A. Jones (each Caltech), and Z.E. Harris for laboratory assistance; C.E. Farnsworth, M. Vondrus, A.P. Kositsky, A.M. Cody (each Caltech), J.B. Miller (USBR), T. McDaniel, and Z.E. Harris for field assistance; and L.E. Bryant (Virginia Tech), C.E. Farnsworth (Caltech), L. Roberts, B. Wehrli, M. Schirmer (each Eawag), A. Voegelin (ETHZ), and M. Krom (Leeds University) for key thoughts during data interpretation. This work was funded by NSF SGER grants EAR-0408329 and EAR-0621371, the Alice Tyler Foundation, USBR grant 06PG400222, and the Carolyn Ash Summer Undergraduate Research Fellowship awarded to Nathan Chan at Caltech. Some sampling resources were provided by Glen Canyon National Recreation Area. The use of trade names is for identification purposes only and does not imply endorsement by the United States National Park Service.

Abstract –

At Lake Powell (a large reservoir in Utah and Arizona, United States of America), we collected high-resolution porewater samples before and after shoreline sediment was exposed to air and subsequently resubmerged by changing water levels. Using porewater manganese as a redox indicator, we observed subsurface reduction conditions in two separate locations before sediment was exposed to air. Non-zero dissolved manganese concentrations existed in samples collected after exposure to air and resubmergence by rising water level, despite our expectation that manganese-oxide precipitation would occur during low water levels due to microbially-mediated oxidation. Thus, the two locations appear to re-establish reducing conditions at different rates, with one location showing high dissolved manganese concentrations just below the surface only 3.5 days after resubmergence, whereas another location showed only moderately increased dissolved manganese after 11.5 days. The difference between the two sites may be explained by differences in local topography, with the former sampling location possibly receiving greater groundwater flow from a nearby hill than the latter location. Uranium data correspond to redox trends with depth in one sampling location. This suggests that this element can be a viable *in situ* redox indicator under certain conditions and that it responds more slowly to the onset of reducing conditions than manganese. Correlations between porewater manganese, arsenic, and lead were observed, indicating that redox conditions may influence the solubility of other trace elements at Lake Powell.

Introduction

The redox geochemistry of trace metals in sediment porewater has been extensively examined in studies both of early diagenesis (e.g., Froelich et al. 1979, Hyacinthe et al. 2001, Katsev et al. 2007) and of the behavior of trace contaminants in shallow groundwater and the hyporheic zone (e.g., Campbell et al. 2008a, Merritt and Amirbahman 2007). Reducing conditions in sediment porewater result from the microbial mineralization of organic carbon and the concomitant respiration of terminal electron acceptors (TEAs). The sequence in which TEAs are utilized generally corresponds to their standard reduction potentials such that the most energetically favorable TEAs, oxygen and nitrate, are reduced first, followed by the reductive dissolution of manganese (Mn) and iron (Fe) oxide minerals, then the reduction of sulfate (SO_4^{2-}) to sulfide (S^{2-}), and finally fermentation reactions (Stumm and Morgan 1996, Hyacinthe et al. 2001). This leads to characteristic depth profiles of the reduced species in porewaters.

Because Mn and Fe oxides often serve as carrier phases for inorganic contaminants such as arsenic (As) and lead (Pb), their reductive dissolution can result in contaminant mobilization and, conversely, their oxidative precipitation in contaminant sequestration (e.g., Campbell et al. 2008b). In addition, the solubility of inorganic contaminants themselves may be controlled by redox conditions. For example, uranium (U) is highly insoluble under reducing conditions, but can be mobile under oxidizing conditions (Wu et al. 2007).

Previous studies of the geochemistry of sediment porewater have focused primarily on lakes and marine basins. In these environments, undisturbed depositional sequences of sediments can be identified, sediments are always fully water-saturated, and advection of

porewater is usually negligible. Redox conditions in lake and marine sediments can change over time in response to changes in the composition of overlying water or the rate and composition of sediment deposition, but the resulting changes in porewater tend to be gradual (Granina et al. 2004, Katsev et al. 2007).

In contrast, shoreline-, tidal flat-, floodplain-, and hyporheic-zone sediments can be exposed to transient conditions associated with changes in water elevation, and they are potentially subject to advective transport (e.g., Baldwin 1996; Beck et al. 2008). In some cases, declining water levels result in exposure of sediments to atmospheric oxygen and the development of unsaturated conditions in the surficial sediments. Drying and rewetting of sediments disturbs ambient redox conditions and may result in changes in porewater redox chemistry (Campbell et al. 2008b), yet the effects of this process have not been extensively examined in field studies.

In this research, depth profiles of TEAs were examined in shoreline sediments subject to changing water levels and exposure to air. Observations before and after sediment exposure and resubmergence are interpreted to provide insight into the *in situ* rate of re-establishment of reducing conditions in porewater, and the effects of changing redox conditions in the sediments on contaminant mobility are examined. These sediments also reflect km-scale heterogeneity associated with spatially varying geology. Samples were collected from locations along the shoreline of Lake Powell, a large reservoir on the Colorado River in Utah and Arizona, where changes in water elevation can be anticipated based on consistent patterns of inflows and outflows. Preliminary surveys of porewater composition indicated that reducing conditions are prevalent in the

surficial shoreline sediments, suggesting that transient exposure to atmospheric oxygen might result in observable changes in porewater geochemistry.

Sampling and Methods

Field site—Lake Powell, a large reservoir on the Colorado River in southeastern Utah and northernmost Arizona, was created in 1963 by the closure of Glen Canyon Dam (Figure 1). Flooding of a dendritic canyon created a reservoir with a long, narrow thalweg and > 90 side canyons that comprise most of the shoreline. Away from the inflows of the Colorado and San Juan Rivers, the shoreline and near-shore lakebed are characterized by sandy sediment deposited by small, intermittent tributaries.

Water releases from Glen Canyon Dam are timed to optimize hydropower production and to fulfill obligations to downstream populations and ecosystems rather than to match inflow to Lake Powell; this reservoir moderates the variable flow of the Colorado River. There is a net loss of reservoir storage between early July and March, followed by a more rapid increase between March and late June, when snowmelt from the Rocky Mountains increases inflows. When yearly inflows and releases are similar in magnitude, this pattern leads to a fluctuation in the water surface elevation of ≤ 8 m. In some years, the increase in storage due to spring runoff does not match the yearly water release, leading to multi-year trends in lake level superimposed on the yearly pattern (Figure 2). All reservoir surface elevations used in this paper are collected by the United States Bureau of Reclamation (http://www.usbr.gov/uc/crsp/GetSiteInfo) at Glen Canyon Dam.

Sample collection—All sampling locations in this study were sandy shorelines that were surrounded by rock. Vegetation was generally very sparse and absent in the areas immediately surrounding the sampling locations. In June 2005, an initial survey of sediment porewater was conducted in White Canyon (WC), Moqui Canyon (MC), the bank of the San Juan River near its inflow (SJ), and Navajo Canyon (NC, Figure 1). Results from the initial survey guided a subsequent field experiment in WC and Farley Canyon (FC). These two side canyons derive most of their sediment from individual rock formations; the Cedar Mesa Sandstone surrounds WC, and the Organ Rock Formation, a shale, surrounds FC (Anderson et al. 2003).

Porewater samples (see below) were collected from FC and WC on 27 January and 28 March 2007 in sediment submerged beneath 10-25 cm of water and located 40-100 cm from the shoreline (Figures 2 and 3). The March sampling location in FC was < 5 m from the January sampling location; in WC, the distance was < 1 m. Multiple samplers were deployed in FC in January (FC-Jan) and March (FC-Mar) and in WC in March (WC-Mar). Sampler FC-Jan-A was located 44 cm from samplers FC-Jan-B and FC-Jan-C, which were 4 cm apart. In January, a single sampler, WC-Jan, was deployed in WC. Samplers FC-Mar-A and FC-Mar-B were separated by 32 cm; samplers WC-Mar-A and WC-Mar-B by 29 cm. The water depth above replicate samplers varied by < 10 cm. In March, > 32 cm-deep sediment cores were collected within 10 cm of each porewater sampler. The FC sampling location was at the base of a small hill (highest point ~8 m above the water level), whereas the WC sampling location was at the end of a flat stretch of sand (highest point ~1 m above the water level).

Sampling and analytical methods—Porewater samples were collected with a constrained "diffusive equilibrium in thin-films" sampler, and gel synthesis followed recently revised methods (Davison et al. 1994, Harper et al. 1997). A 0.45 μm filter membrane separated gel slabs from sediment during deployment, which lasted 20-28 hours according to established sampling methods (Campbell et al. 2008a). Upon removal of the sampler from the sediment, gels were removed from the sampler, transported to the laboratory in polypropylene microcentrifuge tubes, and re-equilibrated in 1% nitric acid (Campbell et al. 2008a). Solutions were diluted and analyzed for Mn, As, U, and Pb on an Agilent 4500 inductively-coupled plasma mass spectrometer (ICP-MS). ICP-MS data were calibrated with multi-element calibration solutions prepared from ICP-grade single element standards for each element (EMD Chemicals, Gibbstown, NJ). Analytical detection limits (μM) were: 0.04 for Mn, 0.008 for U, 0.001 for Pb, and 0.03 for As; relative standard deviations were < 5%.

Sediment cores were collected in 2.5-cm diameter butyrate tubes that were kept cool during transport to the laboratory, frozen ≤ 3 d after collection, and sectioned anoxically at 8 cm intervals. Particle size and chemical analyses of these cores are described elsewhere (Chapter 4). Porosity was measured in the laboratory by adding a known volume of freeze-dried sediment to a known volume of water, measuring the overlying water, and solving

$$\varphi = \frac{V_{w,tot} - V_{w,over}}{(V_{w,tot} - V_{w,over}) + V_{sed}} \qquad (1)$$

where $V_{w,tot}$ is the total volume of water, $V_{w,over}$ is the volume of overlying water after the sediment settles, and V_{sed} is the volume of sediment added. Replicate porosity measurements were made in homogenized sediment core sections 0-4 cm and 8-12 cm

below the SWI in both FC and WC. Any effect of freeze-drying on porosity should be negligible in this sediment because of its large particle size (i.e., the amount of clays that can adsorb water is negligible) and low carbon content (Chapter 4; M. Huettel, Florida State University, personal communication).

Porewater Flux Calculations—When a diffusional gradient of a chemical exists across the sediment-water interface (SWI), the flux from porewater to overlying water can be estimated using

$$J = -\varphi \cdot D_s \cdot \frac{dC}{dz} \qquad (2)$$

where J is flux in μmol L^{-1} cm^{-2} d^{-1}, φ is porosity, D_s is the diffusivity of Mn^{2+} in sediment, expressed in cm^2 s^{-1}, and dC/dz is the vertical concentration gradient, in μmol L^{-1} cm^{-1}. D_s is calculated following Boudreau (1996)

$$D_s = \frac{D_0}{1 - \ln(\varphi^2)} \qquad (3)$$

where D_0, the diffusivity of Mn^{2+} in solution, is adjusted for temperature with the Stokes-Einstein equation,

$$\left(\frac{D\eta}{T}\right)_{T1} = \left(\frac{D\eta}{T}\right)_{T2} \qquad (4)$$

Results

Observations Related to Sediment Transport—The visual appearance of the sediments at each sampling location, observed during repeated field trips, indicated lateral homogeneity on the scale of meters, probably due to isolated sediment-transport events. For example, in WC, a sediment embankment observed on 19 June 2005 was apparently washed away before a return visit on 4-5 December 2005 (Figure 4). The

location of the shoreline in this side canyon was also pushed *downstream* between June and December despite the water elevation being ~49 cm *higher* in December (lake surface elevations = 1097.38 and 1097.87 m above sea level on 19 June and 4 December, respectively), which would be consistent with deposition of the displaced sediment in the streambed. Furthermore, in December 2005, the dry streambed showed evidence of rapid water flow, debris piled on the upstream side of obstructions, and depressions representative of eddies immediately downstream of large rocks. Between the sampling events in January and March 2007, however, there was no evidence of large-scale sediment disturbance in either canyon.

Reservoir Level Fluctuations and Environmental Variables—The surface elevation of Lake Powell varied during this field experiment as a result of different inflows and dam releases. During the 27 January sampling, the reservoir level was at its lowest since the preceding spring, 1097.21 m above sea level (asl), and was falling at ~3.4 cm d^{-1} (Figure 2). By 16 March, continued water level decline led to the yearly minimum, 1096.48 m asl. At the time of the 28 March sampling, 11.5 d later (all times are rounded to 0.5 d), the water surface had risen 34 cm to an elevation of 1096.82 m asl at a rate of ~3.0 cm d^{-1}.

Sediment depths sampled in January had been below the lake surface elevation since May 2006 (Figure 2). After the January sampling, the falling lake level led to similar amounts of time above the water level for the sediment where each sampler was deployed in March: ~26.5 and ~29.0 days for FC-Mar-A and FC-Mar-B, respectively, and ~29.0 and ~20.5 days for WC Mar-A and WC Mar-B, respectively. Upon sampling, the SWI at the locations FC-Mar-A and FC-Mar-B had been resubmerged for 4.0 and 3.5

d, respectively, and the SWI at the locations of WC-Mar-A and WC-Mar-B had been re-submerged for 2.0 and 5.0 d, respectively. The deepest samples of samplers FC-Mar-A, WC-Mar-A, and WC-Mar B were below the minimum reservoir surface elevation in 2007 (henceforth, "low-water line"); these depths had been continuously below the water line since May 2006. The deepest depth sampled by FC-Mar-B was 3.2 cm above the low-water line, so it was above the reservoir water level for 5.0 d and then resubmerged for 10.0 d before sampling.

Daily high air temperature during both sampling events was ~9°C. In January, porewater temperature (T) was 7°C in FC and 5°C in WC. March sampling coincided with a cold front; air T was > 19°C for 3 weeks before dropping the day before sampling. Porewater T was not measured in March, but rapid changes in T are not expected to be translated deep into groundwater (Schmidt et al. 2007). Thus, porewater T can be estimated at 5°C near the SWI and 15°C at depth. Windy conditions during deployment led to overnight accumulation of 5 cm of sediment at the top of samplers WC-Mar-A and WC-Mar-B. However, conditions were calm at the time of sampler retrieval.

At time of sampling, the shoreline near the FC sites were moist even 1-2 m above the water line, whereas the shoreline near the WC sites was mostly dry and disaggregated sand.

Porewater chemistry: overview—Most porewater samples obtained from shoreline sediment at Lake Powell contained Mn and As in concentrations above U.S. Environmental Protection Agency drinking water standards (U.S. EPA 2008). Some samples exceeded the drinking water standard for U, and almost none exceeded the standard for Pb (Table 1).

Porewater chemistry: manganese—Porewater profiles measured from all FC samples and WC-Jan showed approximately similar trends in Mn: concentrations were low in surface water and increased across the SWI to a plateau at depth (Figure 5). WC-Mar samples differed, increasing in Mn concentration below the SWI with no obvious plateau at depth. Maximum Mn concentrations reached 23.8 μmol L^{-1} and 18.6 μmol L^{-1} in FC and WC, respectively. At both sites, small-scale variability with depth was observed in the subsurface. Consistent, low Mn concentrations with depth in the surface water indicated minimal analytical variability.

Profiles from replicate samplers deployed at FC in January and March showed similar variability within consistent ranges. Major trends with depth were similar; fine scale variations with depth did not correspond in the replicate samplers. Porewater profiles at FC and WC differed distinctly between January and March samples with different patterns observed in FC and WC. In FC, maximum concentrations at depth were higher in March than in January, leading to a higher concentration at the sediment-water interface (5.3 μmol L^{-1} versus 1.1 μmol L^{-1} in January) and a steeper gradient (i.e., 1.79 μmol L^{-1} cm^{-1} in FC-Mar-A versus 1.08 μmol L^{-1} cm^{-1} in FC-Jan-A). The opposite was true in WC, where the January profile showed higher values at depth and a steeper gradient than in March (i.e., 2.32 μmol L^{-1} cm^{-1} in WC-Jan versus 0.89 μmol L^{-1} cm^{-1} in WC-Mar-B).

A porosity of 0.45 was measured for all samples. We assume that this value reasonably represents porosity at the sediment surface because 1) the rapid and intermittent sediment deposition at these sites should lead to uniform porosity at depth, and 2) dewatering after sedimentation should remove depth variation due to compaction

by compacting all depths equally on the scale of our porewater measurements. Thus, this value is adequate for use in equation 2. Using the D_0 value of Li and Gregory (1974) and adjusting for temperatures measured in January and estimated in March, $D_s = 1.43 \times 10^{-6}$ $cm^2\ s^{-1}$ in FC and 1.42×10^{-6} $cm^2\ s^{-1}$ in WC in January and 1.42×10^{-6} $cm^2\ s^{-1}$ near the SWI in March. Together with the observed Mn gradients, these values implied fluxes to overlying water of 6.00×10^{-5} μmol Mn^{2+} cm^{-2} d^{-1} in the FC-Jan-A profile, 9.88×10^{-5} µmol Mn^{2+} cm^{-2} d^{-1} in FC-Mar-A, and 1.28×10^{-4} μmol Mn^{2+} cm^{-2} d^{-1} in WC-Jan. In March in WC, gradients across the SWI were negligible, leading to no flux to the overlying water.

Porewater chemistry: uranium—In FC, U concentrations ranged from undetectable to 0.017 μmol L^{-1} in January and 0.005 to 0.025 μmol L^{-1} in March (Figure 6). No samples exceed the drinking water standard of 0.126 µmol L^{-1} (30 μg L^{-1}). Observations of vertical cm-scale variability and replicate profiles resembled those for Mn (described above), though surface water values varied more, suggesting higher analytical variability. Below the SWI, all profiles decreased in concentration from surface maxima, though the January and March profiles changed slope at different depths. In January, concentrations decreased across the SWI to a depth of 5 cm, below which they were constant. However, March concentrations decreased until the low-water line (21 cm), below which they were constant.

Surface water concentrations in WC resembled those of FC, but porewater concentrations were higher (Figure 6). January WC concentrations ranged from 0.003 to 0.065 µM; WC-Mar concentrations were much higher than all other profiles, ranging from 0.015 to 0.13 µmol L^{-1} and exceeding the US EPA standard near the SWI. Unlike

all other profiles, concentrations increased with depth in WC-Jan. Below the SWI, WC-Mar profiles resembled FC-Mar profiles, with concentrations decreasing with depth until the depths of the low-water line at each sampler. Above the SWI, U concentrations in WC-Mar-B decreased sharply over ~4 cm, above which they are constant. A similar trend exists at WC-Mar-A, though the sharp decrease occurs across the SWI, not above it.

Porewater chemistry: lead and arsenic—No trend with depth was observed for Pb or As in January porewater data, and concentration ranges were similar in FC and WC (data not shown). Concentrations of Pb were generally < 0.02 μmol L^{-1}, and As ranged from 0.10 to 0.31 μmol L^{-1}.

In March, Pb concentrations were again < 0.02 μmol L^{-1}, and As concentrations ranged from 0.20 to 0.37 μmol L^{-1} (Figure 7). In FC-Mar-A and FC-Mar-B, concentrations increased across the SWI until a depth of ~11 cm and ~14 cm, respectively, below which they were steady. Trends in WC were small relative to the variability of the data. The trend with depth observed in FC was also observed for As in profile WC-Mar-B, but not in WC-Mar-A.

Discussion

Sediment chemistry—Organic carbon was low (0.03-0.11%), total carbon ranged from 1.0-2.4% and increased with depth, and mineralogical data suggest that the total carbon (C) was mostly carbonate (Chapter 4). Neither parameter showed a statistical difference between FC and WC (t-test, $p < 0.05$), so C was not expected to explain differences in redox chemistry between side canyons. Sediment in FC contained significantly higher Mn, Fe, and Pb than that of WC (t-test, $p < 0.05$); As follows a

similar trend. Concentrations of Mn and Fe in sediment were much higher than those in porewater (Chapter 4) and thus the sedimentary reservoir of these elements was not expected to be depleted.

Scale of sediment deposition and homogeneity—In small, arid washes, sediment is generally transported through brief, intense, "flash" flooding events (Malmon et al. 2004; Prothero and Schwab 2004), which are common on the Colorado Plateau (Dick et al. 1997). Observations during repeated scouting trips to WC in 2005 strongly suggest that a flash flood occurred there in late 2005, moving a substantial amount of sediment downstream such that the shoreline was displaced 1 km down the canyon at a lake level of ~1097 m asl. No such events were observed in FC, yet the close proximity of FC to WC implies that flash floods should also be an important mechanism of sediment transport in that intermittent streambed. Flash flood events are expected to occur energetically and turbulently, leading to spatial homogenization of sediment on the scale of meters, yet not necessarily at the centimeter scale (Prothero and Schwab 2004). This implies that major trends in porewater chemistry measured in replicate samplers should be comparable. However, minor, random, cm-scale variations in both the horizontal and vertical directions could be expected in all sampling locations.

Groundwater advection—During low reservoir levels at Lake Powell, groundwater stored in sediment and rock formations along its banks flows into the reservoir (Potter and Drake 1989). Although we have no data that directly pertain to groundwater advection, estimations are possible based on the slope of the shoreline and the sediment particle size. Sediment from side canyons of Lake Powell consists mostly of sand. The mean values of mean particle sizes measured in multiple samples were 142 and 106 μm

in WC and FC, respectively (samples WC E, 0-8 and 16-24 cm and FC B, 0-8 and 16-24 cm reported in Chapter 4). Since this sediment is well-sorted, the intrinsic permeability (k) can be estimated following an empirical relationship presented by Bear (1972):

$$k = 0.617 \times 10^{-11} \cdot s_{mean} \quad (5)$$

where s_{mean} is the mean particle size of the sediment. From the values reported in Chapter 4, intrinsic permeabilities are estimated at 8.75×10^{-10} cm^2 and 6.52×10^{-10} cm^2 for WC and FC, respectively. These values can be used to calculate hydraulic conductivity (K) using

$$K = k \cdot \frac{\rho \cdot g}{\mu} \quad (6)$$

where ρ is the density of water (in g cm^{-3}), g is gravitational acceleration (980 cm s^{-1}), and μ is the viscosity of water (in g cm^{-1} s^{-1}; Bear 1972). Both the density and viscosity of water were calculated for temperatures of 5°C for WC in January, 7°C for FC in January, and 15°C for both canyons in March. Thus, hydraulic conductivities are estimated to be 5.7×10^{-5} cm s^{-1} and 7.5×10^{-5} cm s^{-1} for WC in January and March, respectively, and 4.5×10^{-5} cm s^{-1} and 5.6×10^{-5} cm s^{-1} for FC in January and March, respectively.

We can estimate the maximum groundwater advection (ω) from the banks of the side canyons into the reservoir by using the slope of the ground surface as the slope of the water table in the equation

$$\omega = K \cdot \frac{dh}{dl} \quad (7)$$

where dh is the difference in groundwater elevations and dl is the length of flow along the groundwater flowpath (Santos et al. 2009). Using the slope of the land at each porewater sampling location and the values of hydraulic conductivity calculated for each sampling

location and time, groundwater advection is estimated to be 3.5×10^{-5} cm s^{-1} and 1.2×10^{-5} cm s^{-1} for WC in January and March, respectively, and 1.4×10^{-5} cm s^{-1} and 1.3×10^{-5} cm s^{-1} for FC in January and March, respectively.

Although these values are slightly more than one order of magnitude larger than the diffusivities calculated for dissolved Mn, they are not directly comparable because advection rates were calculated for groundwater flow in the banks of the reservoir, not at the sampling locations. On one hand, it is possible that this advection may influence the porewater sampling locations, and this influence could not only vary with depth due to cm-scale variations in hydraulic conductivity (thus leading to some of the small-scale variability in the porewater profiles) but also influence the shape of the major trends in the porewater profiles. Conversely, while the above calculation results from the maximum possible hydraulic head that could have existed in the exposed shoreline, the porewater samplers were located in submerged sediment, where we assume no variations in hydraulic head exist. Furthermore, porewater samplers were located > 40 cm from the shoreline, and it is unclear to what extent groundwater flow in the banks of the reservoir could have decreased by groundwater discharge out the sediment surface both above the water level and between the shoreline and the sampling locations. It is also possible that groundwater flow could be less than calculated because of decreased permeability above the water level due to clogging of pore spaces by small particles transported shortly after the decrease in reservoir level. Since the maximum estimated groundwater flow is both not very much greater than the diffusivity of manganese and likely to be much higher than the groundwater flow at the location of the porewater samplers, we tentatively

assume that sediment geochemistry and diffusion, not groundwater advection, are the dominant processes influencing porewater profiles.

Manganese redox chemistry—Concentrations of Mn are used as a porewater redox indicator in this study. Its fast reduction kinetics (Davies and Morgan 1989) make it a good indicator of redox processes on short time scales. Measurements of Mn by ICP-MS are assumed to represent Mn^{2+} due to the low solubility of Mn(III/IV)-oxide compounds.

The similarity of major trends and apparently random, minor, cm-scale variation in porewater Mn observed in replicate samplers is consistent with sediment transport by flash floods. Major trends, such as increases in Mn concentration with depth followed by steadily elevated concentrations, indicate complete consumption of O_2 and reducing conditions just below the SWI. Lateral advection through porewater sampling locations, which could create horizontal redox gradients and confound interpretation of porewater data (Beck et al. 2008), is assumed to be negligible here because side canyon water at Lake Powell is quiescent (Hart et al. 2004), there was no evidence of flow in the FC and WC creeks during this experiment, and the sampling was timed such that the daily lake level change was small.

Variation of $\geq$ 2-5 μmol L^{-1} at the cm-scale has been observed previously due to random, localized sources of solid, reactive organic matter (Shuttleworth et al. 1999; Fones et al. 2001). In this depositional setting, localizations of organic material probably come from decomposing plant debris. Furthermore, cm-scale variation at these sites indicates no physical disruption of sediment. Minor variation with depth may also be due to precipitation of Mn(II) solid minerals, but albandite (MnS) is generally undersaturated in porewater that contains sulfide (Naylor et al. 2006). Rhodocrocite ($MnCO_3$)

precipitation can affect multi-cm trends in Mn and may also vary at the scale of ≤ 1 cm if porewater CO_2 varies at this scale. In this setting, high calcite concentrations are expected to buffer changes in pH that may occur as reducing conditions develop (Masscheleyn et al. 1991).

Similar shapes of Mn profiles collected in both January and March in FC suggest re-establishment of subsurface redox conditions in ≤ 3.5 d after re-flooding. Notably higher concentrations at depth in March are probably attributable to enhanced microbial respiration at higher temperatures. In WC, Mn porewater profiles measured in March samples have lower concentrations than those measured in January samples, and they increase in concentration for several cm below the SWI. These observations indicate that, unlike FC, reducing conditions were not fully re-established in the sediment porewater of WC. These rates of re-establishment are comparable to another study that shows steady-state porewater Mn^{2+} after 3 d in laboratory column experiments (Masscheleyn et al. 1991).

A key assumption underlying this interpretation is that Mn^{2+} was oxidized during sediment exposure. In between the sampling events, the sediment sampled in March is expected to receive oxygen by exposure to air during unsaturation at times of low reservoir level and by reflooding of oxygenated surface water from a rising reservoir. Thermodynamic calculations show that oxidative precipitation of dissolved Mn is highly favorable in the presence of small concentrations of oxygen (Stumm and Morgan 1996), and microbially-mediated oxidation of Mn^{2+} has been observed to occur on a time scale of hours in an air-equilibrated solution (Bargar et al. 2000). Furthermore, U data (discussed below) suggest that oxidizing conditions occurred when the sediment was

above the water line. Thus, we expect that substantial oxidiation of Mn^{2+} would have occurred in unsaturated sediment exposed by the minimum reservoir levels experienced during the study period.

The difference in the rates of *in situ* Mn(III/IV) reduction between FC and WC may be explained by the varying topography at the sampling locations. The wet sediment surface above the water line in FC suggests that groundwater flow from the hill discharged to the sediment surface, keeping it wet several weeks after exposure to air. However, the dry sediment in WC indicates that this did not occur there. This difference may have led to more complete unsaturation and aeration of the sediment matrix in WC during low water levels and better infiltration of oxygenated surface water after re-flooding. This enhanced supply of oxygen would support microbial respiration in sediment porewater, slowing the development of reducing conditions and the subsequent release of Mn^{2+} to the dissolved phase. This difference between side canyons may be augmented by the slightly higher hydraulic conductivity in WC as compared to FC. The larger particle size in WC, which leads to the larger hydraulic conductivity, may result from the different rock formations surrounding the two canyons, implying that local geology may influence the response of porewater chemistry to changing reservoir levels. Other variables, such as sediment chemistry and limnological trends, do not explain the difference between FC and WC: solid-phase C concentrations are similar, solid-phase Mn concentrations far exceed those in porewater, and these side canyons enter the main channel of Lake Powell 0.5 km apart, so they should experience similar trends in lake level and water chemistry. We did not characterize the microbial populations, which might be different in the two canyons. Variations in iron and manganese mineralogy,

which may affect the respiration of chemoautotrophic bacteria, may also contribute to differences in porewater chemistry between FC and WC.

The accumulation of sediment on the samplers deployed in March in WC does not seem to have affected porewater profiles of Mn. These samplers require < 1 h to equilibrate with the sediment porewater (Davison et al. 1994), so this observation implies that a few hours is too short a time for porewater chemistry to change after a rapid sedimentation event.

Our porewater trends differ from those reported from marine basins. In other settings, Mn^{2+} gradients are steeper (e.g., Froelich et al. 1979; Fones et al. 2001; Hyacinthe et al. 2001), resulting in diffusive fluxes an order of magnitude higher than those reported here, which are on par with another shoreline study (Table 2). This difference may result from the rapid, intermittent sedimentation at our field location and the rapid sedimentation at the site of Campbell et al. (2008b). In our Mn profiles, concentrations increase sharply across the SWI, whereas Mn concentration gradients reported by studies of marine basins and that of Campbell et al. (2008b) occur below the SWI. The shallow placement of our Mn gradients may result from high sedimentation rate (Granina et al. 2004) or more reactive organic C in our sediment.

Uranium chemistry—Profiles of porewater U can add to an interpretation of redox geochemistry based on Mn. In oxidizing conditions, carbonate generally complexes UO_2^{2+} in the dissolved phase; upon reduction, solid uraninite (UO_2) precipitates (Wu et al. 2007). Porewater U measured in January in FC suggest that U reduction appears to occur concomitantly with Mn reduction, since the concentrations of these elements anticorrelate with depth. This is consistent with groundwater bioremediation and laboratory studies,

which show that low levels of Mn(III/IV)- and Fe(III)-oxide minerals oxidize U(IV) and thus frequently control its mobility in groundwater (Tokunaga et al. 2008; Fredrickson et al. 2008). In March, however, the steady decrease of U concentrations from the SWI to near the low-water line and constant concentration below this depth imply that U was oxidized when the sediment was unsaturated in between the sampling times. This agrees with a groundwater biostimulation study in which the onset of reducing conditions led to nearly complete reduction and precipitation of U(IV) and subsequent introduction of dissolved oxygen promptly oxidized and dissolved U solids (Wu et al. 2007). In FC, the higher concentrations of porewater U above the low-water line in March relative to January suggest that further U reduction may have been possible after the March sampling event, which may have captured an ongoing process. This differs from the porewater Mn observations and suggests that, after exposure to oxygen and re-flooding, reduction of U(VI) may occur at a slower rate than that of Mn(IV).

In WC in January, an increase of porewater U with depth, despite reducing conditions indicated by Mn, may imply that U is complexed in solution, perhaps by dissolved organic carbon (Wan et al. 2008), or (bi)carbonate (Ginder-Vogel et al. 2006). Such complexation would depend on pH and the type and amount of Fe(III)-oxides present (Stewart et al. 2007), yet quantification of this reaction is not possible since porewater pH, dissolved carbonate, and detailed iron mineralogy data were not collected as part of this study. While our data do not allow conclusions about the mechanism causing the observed depth profiles of U, they show that, whereas U and Mn reduction occur in concert in FC, these reactions are controlled by separate processes in WC.

Despite the slow onset of reducing conditions in WC after sediment exposure and re-flooding, U concentrations decrease with depth below the SWI, suggesting that the onset of reducing conditions after resubmergence may affect both Mn and U. High subsurface concentrations suggest that, as in FC, sediment exposure oxidized and mobilized U. Higher concentrations in WC than in FC may be a result of the legacy of U mining in the WC catchment from 1948-1954 (Farmer 1999).

Lead and arsenic—In sediment porewater, Pb and As are known to correspond to trends in redox chemistry. In FC and WC, variations with depth are nonexistent or small (i.e., in FC in March) and only generally correspond to Mn trends, suggesting that Mn-oxide minerals may not be dominant sorbents of As and Pb in this setting. Instead, As and Pb are probably sorbed to Fe minerals, which occur at this site and commonly sorb trace elements. In samples collected across Lake Powell in an initial survey of porewater conditions, correlations are most consistent between porewater Mn and Pb (Table 3). When considered along with the detailed results collected in FC and WC, this preliminary finding suggests that porewater redox chemistry plays a role in trace contaminant mobility in different regions of the Lake Powell shoreline.

Implications—The yearly rise and fall of the surface elevation at Lake Powell is a result of the snowmelt-dominated runoff of the Colorado River and dam operation that prioritizes hydropower production and downstream water supply. When the surface elevation of Lake Powell is steady or falling slightly, Mn diffuses out of shoreline sediment submerged under < 30 cm of water. This observation, which is not common among studies of porewater diagenesis, may be attributed to sporadic deposition of organic C associated with sedimentation that occurs due to flash floods. This process

could impair water quality as concentrations of Mn and As in porewater frequently exceed drinking water standards, although elevated Mn concentrations in the overlying water occur only just above the SWI. This is unlikely to pose a public health threat, since water in Lake Powell side canyons is extremely low in trace metals due to dilution (Hart et al. 2004) and most recreational visitors to shorelines at Lake Powell are expected to be exposed to porewater only through dermal contact. Porewater U may be enhanced in White Canyon due to the mining legacy of that catchment.

We know of no other study that reports high-resolution, *in situ*, porewater profiles of redox-active elements during non-equilibrium conditions such as the ones imposed at the shoreline of Lake Powell during yearly variation in lake level. Upon re-flooding, redox gradients are re-established at rates that may differ based on sediment permeability, which may relate to the local geology in specific regions of the shoreline. During a slow rise in lake level, it appears unlikely that Mn diffusion out of sediment will occur at all shoreline locations.

Our data also suggest that, under certain conditions, uranium may be a useful redox indicator in shallow porewater and that the comparisons of manganese and uranium profiles may provide insight into the response of a system to changing redox conditions. Our results suggest that reduction of Mn(IV/III) is more facile than that of U(VI), which is consistent both with the thermodynamics of the reactions and the results of laboratory and groundwater biostimulation studies.

References

Anderson, P. B., T. C. Chidsey, D. A. Sprinkel, and G. C. Willis. Geology of Glen Canyon National Recreation Area, Utah-Arizona. 2003. *In* D. A. Sprinkel, T. C.

Chidsey, and P. B. Anderson [eds.], Geology of Utah's Parks and Monuments, 2nd ed. Utah Geological Association.

Baldwin, D. S. 1996. Effects of exposure to air and subsequent drying on the phosphate sorption characteristics of sediments from a eutrophic reservoir. Limnol. Oceanogr. 41: 1725-1732.

Bargar, J. R., B. M. Tebo, and J. E. Villinski. 2000. In situ characterization of Mn(II) oxidation by spores of the marine *Bacillus* sp. strain SG-1. Geochim. Cosmochim. Acta 64: 2775-2778.

Bear, J. *Dynamics of fluids in porous media.* Dover Publications, Inc.: Mineola, NY, 1972.

Beck, M., O. Dellwig, B. Schnetger, and H.-J. Brumsack. 2008. Cycling of trace metals (Mn, Fe, Mo, U, V, Cr) in deep pore waters of intertidal flat sediments. Geochim. Cosmochim. Acta 72: 2822-2840.

Berner, R. A. 1980. Early Diagenesis: A Theoretical Approach. Princeton University Press.

Boudreau, B. P. 1996. The diffusive tortuosity of fine-grained unlithified sediments. Geochim. Cosmochim. Acta 60: 3139-3142.

Campbell, K. M., R. Root, P. A. O'Day, and J. G. Hering. 2008a. A gel probe equilibrium sampler for measuring arsenic porewater profiles and sorption gradients in sediments: 1. Laboratory development. Environ. Sci. Technol. 42: 497-503.

Campbell, K. M., R. Root, P. A. O'Day, and J. G. Hering. 2008b. A gel probe equilibrium sampler for measuring arsenic porewater profiles and sorption gradients in sediments: II. Field application to Haiwee Reservoir sediment. Environ. Sci. Technol. 42: 504-510.

Davies, S. H. R. and J. J. Morgan. 1989. Manganese(II) oxidation kinetics on metal oxide surfaces. J. Col. Int. Sci. 129: 63-77.

Davison, W., H. Zhang, and G. W. Grime. 1994. Performance characteristics of gel probes used for measuring the chemistry of pore waters. Environ. Sci. Technol. 28: 1623-1632.

Dick, G. S., R. S. Anderson, and D. E. Sampson. 1997. Controls on flash flood magnitude and hydrograph shape, Upper Blue Hills badlands, Utah. Geology 25: 45-48.

Farmer, J. 1999. Glen Canyon Dammed: Inventing Lake Powell and the Canyon Country. The University of Arizona Press.

Fones, G. R., W. Davison, O. Holby, B. B. Jorgensen, and B. Thamdrup. 2001. High-resolution metal gradients measured by *in situ* DGT/DET deployment in Black Sea sediments using an autonomous benthic lander. Limnol. Oceanogr. 46: 982-988.

Fredrickson, J. K., J. M. Zachara, D. W. Kennedy, C. Liu, M. C. Duff, D. B. Hunter, and A. Dohnalkova. 2008. Influence of Mn oxides on the reduction of uranium(VI) by the metal-reducing bacterium Shewanella putrefaciens. Geochim. Cosmochim. Acta 66: 3247-3262.

Froelich, P. N., G. P. Klinkhammer, M. L. Bender, N. A. Luedtke, G. R. Heath, D. Cullen, P. Dauphin, D. Hammond, B. Hartman, and V. Maynard. 1979. Early oxidation of organic matter in pelagic sediments of the eastern equatorial Atlantic: suboxic diagenesis. Geochim. Cosmochim. Acta 43: 1075-1090.

Ginder-Vogel, M., C. S. Criddle, and S. Fendorf. 2006. Thermodynamic constraints on the oxidation of biogenic UO_2 by Fe(III) (Hydr)oxides. Environ. Sci. Technol. 40: 3544-3550.

Granina, L., B. Muller, and B. Wehrli. 2004. Origin and dynamics of Fe and Mn sedimentary layers in Lake Baikal. Chem. Geol. 205: 55-72.

Harper, M. P., W. Davison, and W. Tych. 1997. Temporal, spatial, and resolution constraints for *in situ* sampling devices using diffusional equilibrium: dialysis and DET. Environ. Sci. Technol. 31: 3110-3119.

Hart, R. J., H. E. Taylor, R. C. Antweiler, G. G. Fisk, G. M. Anderson, D. A. Roth, M. E. Flynn, D. B. Pearl, M. Truini, and L. B. Barber. 2004. Physical and chemical characteristics of Knowles, Forgotten, and Moqui Canyons, and effects of recreational use on Water Quality, Lake Powell, Arizona and Utah. United States Geol. Surv. Sci. Inv. Rep. 2004-5120.

Hyacinthe, C., P. Anschutz, P. Carbonel, J.-M. Jouanneau, and F. J. Jorissen. 2001. Early diagenetic processes in the muddy sediments of the Bay of Biscay. Mar. Geol. 177: 111-128.

Katsev, S., G. Chaillou, B. Sundby, and A. Mucci. 2007. Effects of progressive oxygen depletion on sediment diagenesis and fluxes: A model for the lower St. Lawrence River Estuary. Limnol. Oceanogr. 52: 2555-2568.

Kneebone, P. E. 2000. Arsenic geochemistry in a geothermally impacted system: The Los Angeles Aqueduct. Ph.D. thesis. Calif. Inst. of Tech.

Li, Y.-H. S. Gregory. 1974. Diffusion of ions in sea water and in deep-sea sediments. Geochim. Cosmochim. Acta 38: 703-714.

Malmon, D. V., S. L. Reneau, and T. Dunne. 2004. Sediment sorting and transport by floods. J. Geophys. Res. 109: F02005, doi:10.1029/2003JF000067.

Masch, F. D. and K. J. Denny. 1966. Grain size distribution and its effect on the permeability of unconsolidated soils. Wat. Resour. Res. 2: 665-677.

Masscheleyn, P. H., R. D. Delaune, and W. H. Patrick, Jr. 1991. Effect of redox potential and pH on arsenic speciation and solubility in a contaminated soil. Environ. Sci. Technol. 25: 1414-1419.

Merritt, K. A. and A. Amirbahman. 2007. Mercury dynamics in sulfide-rich sediments: Geochemical influence on contaminant mobilization within the Penobscot River estuary, Maine, USA. Geochim. Cosmochim. Acta 71: 929-941.

Naylor, C., W. Davison, M. Motelica-Heino, G. A. van den Berg, L. M. van der Heijdt. 2006. Potential kinetic availability of metals in sulphidic freshwater sediments. Sci. Tot. Environ. 357: 208-220.

Potter, L. D. and C. L. Drake. *Lake Powell: Virgin Flow to Dynamo.* University of New Mexico Press, Albuquerque, 1989.

Prothero, D.R. and F. Schwab. 2004. Sedimentary Geology, 2nd ed. Freeman.

Schmidt, C., B. Conant, Jr., M. Bayer-Raich, and M. Schirmer. 2007. Evaluation and field-scale application of an analytical method to quantify groundwater discharge using mapped streambed temperatures. J. Hydrol. 357: 292-307.

Shuttleworth, S. M., W. Davison, and J. Hamilton-Taylor. 1999. Two-dimensional and fine structure in the concentrations of iron and manganese in sediment pore-waters. Environ. Sci. Technol. 33: 4169-4175.

Stewart, B. D., J. Neiss, and S. Fendorf. 2007. Quantifying constraints imposed by calcium and iron on bacterial reduction of uranium(VI). J. Environ. Qual. 36: 363-372.

Stumm, W. and J. J. Morgan. 1996. Aquatic Chemistry, 3rd ed. Wiley.

Tokunaga, T. K, J. Wan, Y. Kim, S. R. Sutton, M. Newville, A. Lanzirotti, and W. Rao. 2008. Real-time x-ray absoption spectroscopy of uranium, iron, and manganese in contaminated sediments during bioreduction. Environ. Sci. Technol. 42: 2839-2844.

United States Environmental Protection Agency. 2008. Drinking Water Contaminants. Webpage viewed on 14 December 2008 at http://www.epa.gov/safewater/contaminants/index.html#listmcl.

Wan, J., T. K. Tokunaga, Y. Kim, E. Brodie, R. Daly, T. C. Hazen, and M. K. Firestone. 2008. Effects of organic carbon supply rates on uranium mobility in a previously bioreduced contaminated sediment. Environ. Sci. Technol. 42: 7573-7579.

Wu, W.-M., J. Carley, J. Luo, M. A. Ginder-Vogel, E. Cardenas, M. B. Leigh, C. Hwang, S. D. Kelly, C. Ruan, L. Wu, J. van Nostrand, T. Gentry, K. Lowe, T. Mehlhorn, S. Carroll, W. Luo, M. W. Fields, B. Gu, D. Watson, K. M. Kemner, T. Marsh, J. Tiedje, J. Zhou, S. Fendorf, P. K. Kitanidis, P. M. Jardine, and C. S. Criddle. 2007. In situ bioreduction of uranium (VI) to submicromolar levels and reoxidation by dissolved oxygen. Environ. Sci. Technol. 41: 5716-5723.

Tables

Table 1. Trace elements in sediment porewater sampled at the Lake Powell shoreline

element	Mn	U	Pb	As
EPA standard[a,b]	0.91	0.13	0.072	0.13
Farley Canyon				
median[a]	7.0	0.005	0.009	0.22
standard deviation[a]	4.2	0.005	0.009	0.32
number of samples	207	207	203	203
% above standard	100	0	1	100
White Canyon				
median[a]	8.3	0.048	0.012	0.22
standard deviation[a]	5.5	0.030	0.016	0.28
number of samples	197	198	198	120
% above standard	97	0	1	98
Moqui Canyon				
median[a]	1.8	0.006	0	
standard deviation[a]	5.6	0.006	0.03	
number of samples	53	53	53	
% above standard	91	0	6	
San Juan River				
median[a]	0	0.03	0.04	
standard deviation[a]	14	0.003	0.06	
number of samples	53	53	53	
% above standard	45	0	17	
Navajo Canyon				
median[a]	3.7	0.08	0.03	
standard deviation[a]	3.3	0.001	0.02	
number of samples	53	53	53	
% above standard	87	0	6	97

[a] Concentrations in μM.

[b] Primary drinking water standards for U, Pb, As; secondary drinking water standard for Mn (US EPA 2008)

Table 2. Porewater Mn^{2+} flux across the sediment-water interface[a]

porosity	T (K)	dC/dz	flux[b]	source[c]
0.45	278	-2.3	0.047	(1)
0.45	278	-1.6	0.012	(2)
0.45	278	-1.8	0.036	(3)
0.61[d]	298	-4.8	0.19	(4)
?[e]	280	-10.5	0.50	(5)
			0.2	(6)
			2.6	(6)
?[f]	?[f]		4.5	(6)
			5.6	(6)
			6.2	(6)

[a] Fluxes for Cambell et al. (2008b) and Fones et al. (2001) calculated from ideal Mn2+ diffusivity and porewater profiles in their figures.

[b] in μmol cm^{-2} d^{-1} or μmol cm^{-2} yr^{-1}

[c] References: 1: WC-Jan-A (this study), 2: FC-Jan-A (this study), 3: FC-Mar-A (this study), 4: Campbell et al. 2008b, 5: Fones et al. 2001, 6: Hyacinthe et al. 2001

[d] Porosity from Kneebone (2000).

[e] Porosity not reported, estimated at 0.7.

[f] Porosity and temperature not reported for all fluxes reported by Hyacinthe et al. (2001).

Table 3. Correlations[a] of solutes with Mn

location	month	U	Pb	As	n
FC	01/07		0.087	**0.211**	161
FC	03/07	**-0.705**	**0.482**	**0.855**	121
WC	01/07		0.070	-0.087	46
WC	03/07	**0.282**	0.059	**0.388**	101
WC	06/05	0.176	**0.842**		79
NC	06/05	-0.001	**0.946**		43
SJ	06/05	0.085	**0.972**		54
MC	06/05	0.028	**0.946**		53

[a] Bold text indicates $p < 0.05$, underline indicates $p < 0.0001$.

Figure Captions

Figure 1. Map of Lake Powell. Water flows through the reservoir from the northeast to the southwest, where it passes through Glen Canyon Dam (GCD). The Colorado River arm is north of the San Juan River arm. Other abbreviations indicate sampling locations as described in the text. The black box in the inset represents the area covered by the map.

Figure 2. Lake Powell water surface elevation above sea level. *Left panel*: 1997-2007; the box highlights the time range in the right panel. *Right panel*: 1 December 2006 to 1 December 2007; the box shows the sampling period for this study.

Figure 3. Sample deployment in White Canyon. Vertical rectangles indicate locations of samplers WC-Jan, WC-Mar-A, and WC-Mar-B from left to right. The intersection of the each sampler with the sediment-water interface (SWI) is shown. Dashed horizontal lines represent reservoir levels, including the low-water line during the experiment (see text). Sample deployment in Farley Canyon was similar.

Figure 4. Qualitative evidence of sediment transport in WC. Above: Side view photograph taken 5 December 2005. The white dashed line shows the approximate extent of a sediment embankment observed on 19 June 2005. A person (1.8 m tall) is in the white oval for scale. Left: Map view. Arrows, located in the streambed, indicate direction of intermittent flow. Solid lines show approximate shoreline location in June (upstream) and December (downstream) at the same reservoir elevation. Crescent formed by dashed lines shows the estimated extent of sediment removal from the embankment in the side

view. Person in side view is standing at the June shoreline location. Upper image courtesy Andrew Kositsky, Caltech; lower image from Google Earth.

Figure 5. Porewater profiles of Mn concentrations in Farley Canyon (left panel) and White Canyon (right panel) as a function of depth in the sediment where zero depth corresponds to the sediment-water interface (SWI) and negative depths correspond to the height above the SWI. Samples were collected before (Jan) and after (Mar) exposure and re-submergence of shoreline sediment. Solid horizontal lines indicate the lowest water elevation between January and March relative to the SWI on the sampling date of samplers FC-Mar-A, WC-Mar-A (gray line), and WC-Mar-B (black line). These lines occur at different depths because replicate samplers were inserted into sloping sediment and these graphs are normalized to the SWI. In the left panel, running averages of replicate samplers are displayed. In the right panel, the dashed line above the SWI shows the depth of sedimentation that occurred during sampler deployment in March.

Figure 6. Porewater profiles of U concentrations in Farley Canyon (left panel) and White Canyon (right panel) as a function of depth in the sediments where zero depth corresponds to the sediment-water interface (SWI) and negative depths correspond to the height above the SWI. Note the difference in scale between the two panels. Samples were collected before (Jan) and after (Mar) exposure and re-submergence of shoreline sediment. Solid horizontal lines indicate the lowest water elevation between January and March relative to the SWI on the sampling date of samplers FC-Mar-A, WC-Mar-A (gray line), and WC-Mar-B (black line). These lines occur at different depths because replicate

samplers were inserted into sloping sediment and these graphs are normalized to the SWI. In the left panel, running averages of replicate samplers are displayed. In the right panel, the dashed line above the SWI shows the depth of sedimentation that occurred during sampler deployment in March.

Figure 7. Porewater profiles of Pb (triangles and diamonds) and As (circles and squares) concentrations in Farley Canyon (left panel) and White Canyon (right panel) as a function of depth in the sediments where zero depth corresponds to the sediment-water interface (SWI) and negative depths correspond to the height above the SWI. Note the difference in scale between the two panels. Samples were collected before (Jan) and after (Mar) exposure and re-submergence of shoreline sediment. Solid horizontal lines indicate the lowest water elevation between January and March relative to the SWI on the sampling date of samplers FC-Mar-A, WC-Mar-A (gray line), and WC-Mar-B (black line). These lines occur at different depths because replicate samplers were inserted into sloping sediment and these graphs are normalized to the SWI. In the right panel, the dashed line above the SWI shows the depth of sedimentation that occurred during sampler deployment in March.

Figure 1

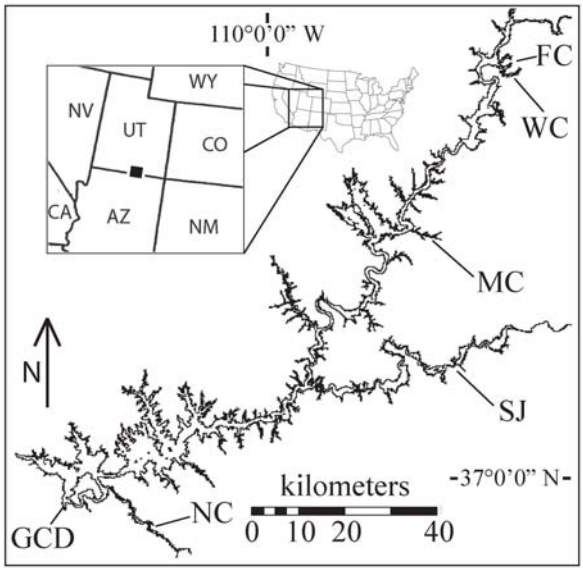
110°0'0" W
WY
NV
UT
CO
CA
AZ
NM
FC
WC
MC
N
SJ
kilometers
-37°0'0" N-
NC
GCD
0 10 20 40

Figure 2

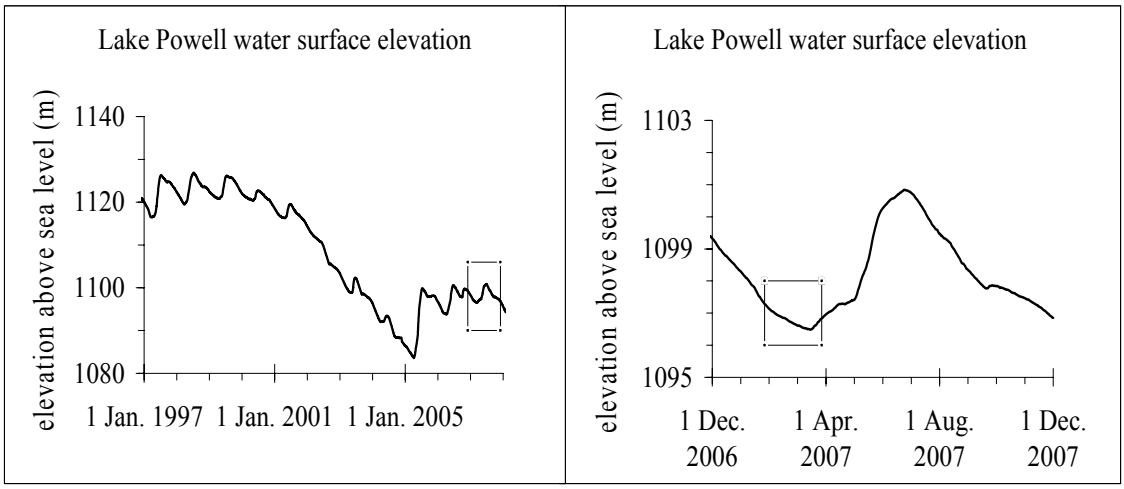
Lake Powell water surface elevation
elevation above sea level (m)
1140
1120
1100
1080
1 Jan. 1997
1 Jan. 2001
1 Jan. 2005
Lake Powell water surface elevation
elevation above sea level (m)
1103
1099
1095
1 Dec. 2006
1 Apr. 2007
1 Aug. 2007
1 Dec. 2007

Figure 3

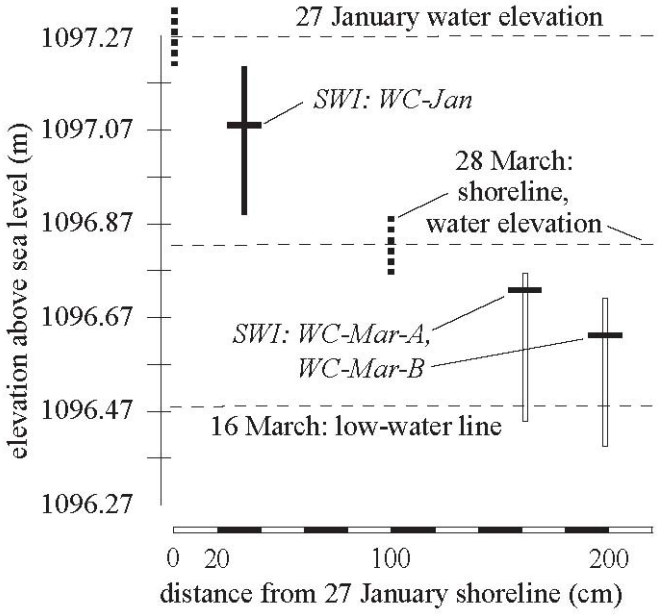
27 January water elevation
1097.27
1097.07
1096.87
1096.67
1096.47
1096.27
elevation above sea level (m)
SWI: WC-Jan
28 March:
shoreline,
water elevation
SWI: WC-Mar-A,
WC-Mar-B
16 March: low-water line
0
20
100
200
distance from 27 January shoreline (cm)

Figure 4

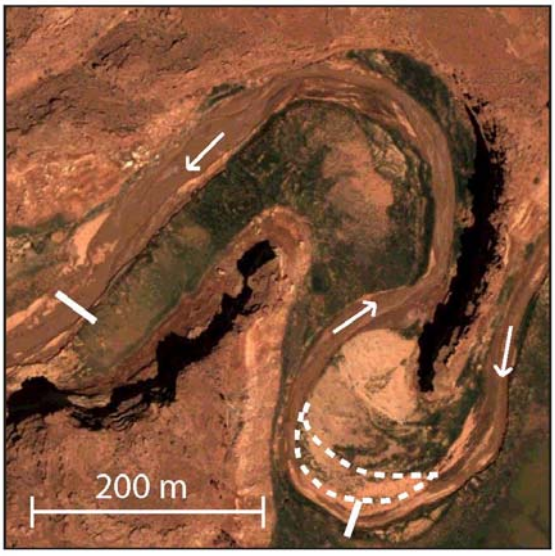

Figure 5

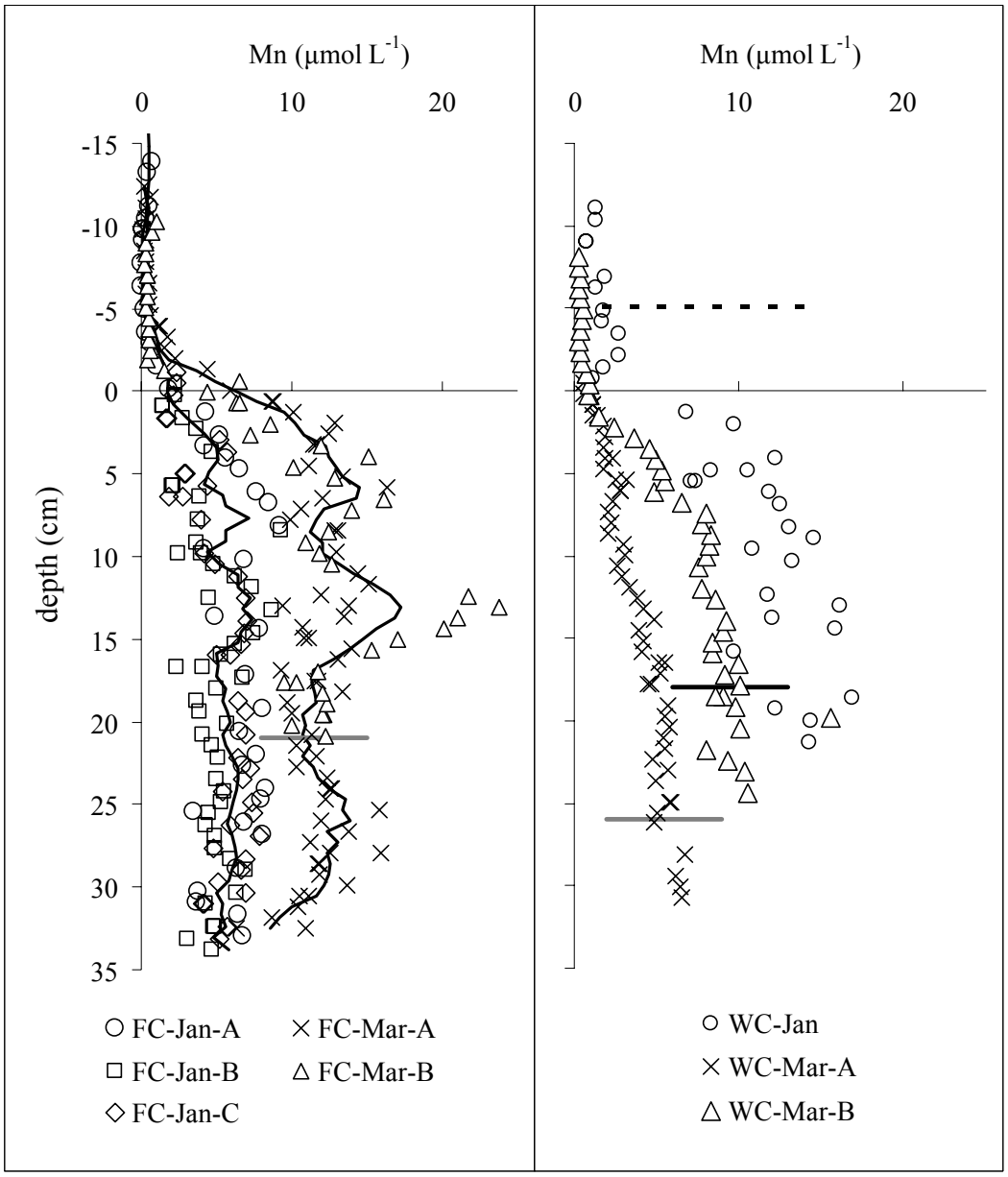
Mn (µmol L-1)
0
10
20
-15
-10
-5
0
5
10
15
20
25
30
35
depth (cm)
FC-Jan-A
FC-Jan-B
FC-Jan-C
FC-Mar-A
FC-Mar-B
Mn (µmol L-1)
0
10
20
WC-Jan
WC-Mar-A
WC-Mar-B

Figure 6

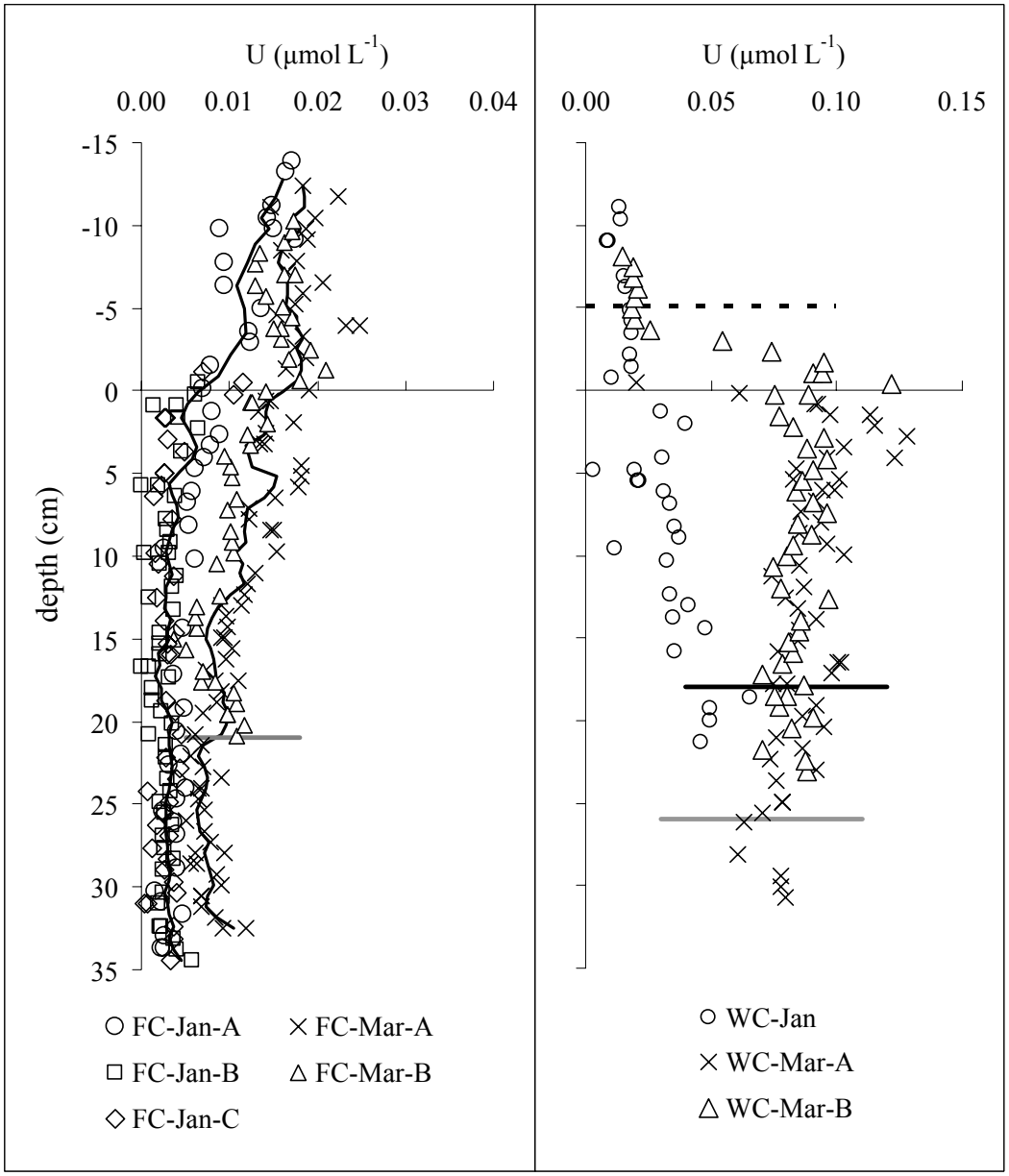
U (µmol L-1)
0.00
0.01
0.02
0.03
0.04
-15
-10
-5
0
5
10
15
20
25
30
35
depth (cm)
FC-Jan-A
FC-Jan-B
FC-Jan-C
FC-Mar-A
FC-Mar-B
U (µmol L-1)
0.00
0.05
0.10
0.15
WC-Jan
WC-Mar-A
WC-Mar-B

Figure 7

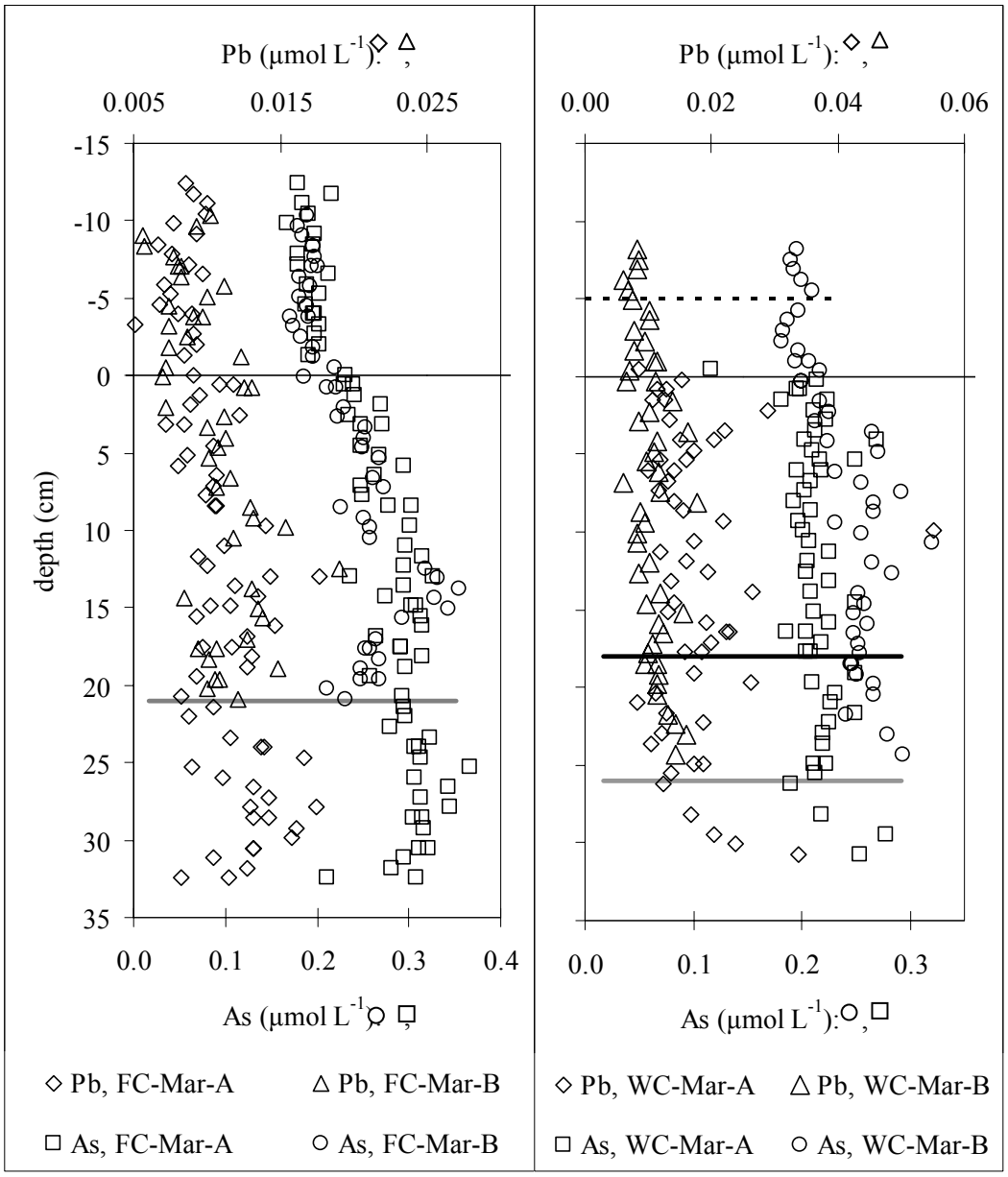
Pb (µmol L-1): ◇, △
0.005
0.015
0.025
-15
-10
-5
0
5
10
15
20
25
30
35
depth (cm)
0.0
0.1
0.2
0.3
0.4
As (µmol L-1): ○, □
◇ Pb, FC-Mar-A
△ Pb, FC-Mar-B
□ As, FC-Mar-A
○ As, FC-Mar-B
Pb (µmol L-1): ◇, △
0.00
0.02
0.04
0.06
0.0
0.1
0.2
0.3
As (µmol L-1): ○, □
◇ Pb, WC-Mar-A
△ Pb, WC-Mar-B
□ As, WC-Mar-A
○ As, WC-Mar-B

Appendix

Table A1. Concentrations (in μM) of manganese (Mn), uranium (U), and lead (Pb) measured during a June 2005 survey of porewater in side canyon sediment of Lake Powell; depth (in cm) of 0 is the sediment-water interface

depth	Mn	U	Pb	depth	Mn	U	Pb
White Canyon				*Moqui Canyon*			
-1.30	11.96	0.041	0.040	-0.65	2.12	0.006	0.039
-0.65	13.82	0.031	0.039	0.00	0.55	0.006	0.031
0.00	9.99	0.020	0.030	0.65	-0.18	0.006	0.030
0.65	10.16	0.021	0.040	1.30	-0.50	0.006	0.029
1.30	12.06	0.042	0.037	1.95	-0.60	0.006	0.029
1.95	13.85	0.023	0.050	2.60	0.13	0.006	0.035
2.60	11.66	0.023	0.041	3.25	-0.08	0.006	0.035
3.25	18.47	0.025	0.041	3.90	-0.18	0.006	0.038
3.90	14.92	0.025	0.049	4.55	0.65	0.006	0.058
4.55	11.72	0.018	0.041	5.20	0.44	0.006	0.056
5.20	12.98	0.020	0.041	5.85	-1.23	0.006	0.032
5.85	12.78	0.019	0.039	6.50	4.11	0.006	0.075
6.50	10.04	0.018	0.048	7.15	7.46	0.006	0.079
7.15	8.91	0.017	0.039	7.80	6.41	0.006	0.070
7.80	12.84	0.020	0.039	8.45	13.65	0.000	0.097
8.45	10.50	0.018	0.042	9.10	22.74	0.006	0.120
9.10	27.09	0.021	0.074	9.75	30.59	0.006	0.140
9.75	17.26	0.023	0.062	10.40	32.89	0.030	0.145
10.40	11.72	0.018	0.060	11.05	11.02	0.030	0.088
11.05	10.51	0.018	0.054	11.70	7.35	0.030	0.068
11.70	8.86	0.018	0.043	12.35	9.13	0.030	0.096
12.35	15.58	0.022	0.080	13.00	4.84	0.030	0.053
13.00	11.72	0.019	0.057	13.65	0.97	0.030	0.039
13.65	13.24	0.019	0.080	14.30	1.81	0.030	0.041
14.30	9.35	0.016	0.041	14.95	0.44	0.030	0.032
14.95	9.76	0.018	0.045	15.60	0.55	0.030	0.032
15.60	10.68	0.020	0.036	16.25	0.44	0.030	0.031
16.25	6.52	0.014	0.026	16.90	0.44	0.030	0.030
16.90	14.61	0.022	0.045	17.55	0.49	0.000	0.030
17.55	11.84	0.029	0.042	18.20	0.55	0.006	0.029
18.20	16.86	0.028	0.056	18.85	0.65	0.030	0.031
18.85	12.00	0.026	0.046	19.50	0.76	0.030	0.029
19.50	7.09	0.020	0.028	20.15	1.60	0.030	0.032
20.15	15.31	0.024	0.071	20.80	0.44	0.006	0.028

Table A1: Concentrations of Mn, U, and Pb in side canyon porewater, continued.

depth	Mn	U	Pb	depth	Mn	U	Pb
White Canyon, continued				*Moqui Canyon, continued*			
20.80	13.08	0.020	0.059	21.45	2.75	0.030	0.035
21.45	9.96	0.021	0.042	22.10	2.12	0.030	0.032
22.10	11.79	0.025	0.039	22.75	0.55	0.030	0.029
22.75	9.10	0.023	0.024	23.40	0.34	0.006	0.030
23.40	9.01	0.025	0.023	24.05	0.65	0.030	0.029
24.05	10.88	0.027	0.033	24.70	0.34	0.006	0.029
24.70	17.98	0.039	0.068	25.35	0.76	0.030	0.028
25.35	18.16	0.033	0.045	26.00	0.24	0.030	0.026
26.00	39.13	0.042	0.107	26.65	0.55	0.006	0.032
27.30	20.11	0.041	0.061	27.30	0.55	0.006	0.028
27.95	17.68	0.034	0.053	27.95	0.44	0.006	0.030
28.60	20.65	0.039	0.050	28.60	0.03	0.030	0.030
29.25	20.87	0.041	0.059	29.25	0.34	0.006	0.028
29.90	25.29	0.052	0.097	29.90	0.03	0.006	0.029
30.55	26.27	0.048	0.122	30.55	0.24	0.006	0.033
31.20	31.33	0.059	0.144	31.20	0.13	0.006	0.029
31.85	25.51	0.048	0.097	31.85	-0.08	0.006	0.030
32.50	17.59	0.038	0.066	32.50	0.34	0.030	0.035
33.15	15.78	0.036	0.076	33.15	1.70	0.030	0.046
33.80	11.40	0.034	0.047	*San Juan River*			
34.45	11.58	0.030	0.049	-0.65	52.68	0.030	0.201
35.10	13.03	0.033	0.051	0.00	66.50	0.030	0.284
35.75	11.52	0.031	0.034	0.65	66.70	0.030	0.340
36.40	10.23	0.028	0.041	1.30	40.95	0.030	0.201
37.05	11.05	0.034	0.043	1.95	29.75	0.030	0.201
37.70	8.01	0.030	0.027	2.60	22.32	0.030	0.146
38.35	10.30	0.039	0.027	3.25	13.11	0.030	0.090
39.00	8.78	0.033	0.034	3.90	7.25	0.030	0.062
39.65	9.32	0.035	0.037	4.55	4.21	0.030	0.062
40.30	10.04	0.036	0.044	5.20	6.52	0.030	0.035
40.95	9.01	0.028	0.044	5.85	3.27	0.030	0.035
41.60	8.55	0.036	0.032	6.50	4.00	0.030	0.062
42.25	7.77	0.034	0.036	7.15	2.64	0.030	0.062
42.90	8.20	0.041	0.025	7.80	1.70	0.030	0.035
43.55	6.83	0.041	0.024	8.45	1.18	0.030	0.035
44.20	8.18	0.040	0.022	9.10	3.59	0.030	0.035
44.85	7.14	0.032	0.031	9.75	1.49	0.030	0.035

Table A1. Concentrations of Mn, U, and Pb in side canyon porewater, continued

depth	Mn	U	Pb	depth	Mn	U	Pb
White Canyon, continued				*San Juan River, continued*			
45.50	10.21	0.062	0.041	10.40	0.65	0.030	0.035
46.15	10.45	0.049	0.026	11.05	2.96	0.030	0.035
46.80	8.88	0.061	0.022	11.70	0.55	0.030	0.035
Navajo Canyon				12.35	3.90	0.030	0.062
47.45	10.39	0.071	0.024	13.00	4.11	0.030	0.035
48.10	13.17	0.080	0.029	13.65	2.22	0.030	0.035
48.75	8.18	0.077	0.024	14.30	5.78	0.030	0.035
49.40	6.33	0.059	0.028	14.95	3.90	0.030	0.035
50.05	6.85	0.040	0.043	15.60	6.20	0.030	0.035
-0.65	2.12	0.006	0.039	16.25	2.22	0.030	0.035
0.00	0.55	0.006	0.031	16.90	1.60	0.030	0.035
0.65	-0.18	0.006	0.030	17.55	0.76	0.006	0.035
1.30	-0.50	0.006	0.029	18.20	3.27	0.030	0.035
1.95	-0.60	0.006	0.029	18.85	3.59	0.030	0.035
2.60	0.13	0.006	0.035	19.50	2.64	0.030	0.035
3.25	-0.08	0.006	0.035	20.15	6.10	0.030	0.035
3.90	-0.18	0.006	0.038	20.80	7.25	0.030	0.035
4.55	0.65	0.006	0.058	21.45	15.62	0.030	0.090
5.20	0.44	0.006	0.056	22.10	6.20	0.030	0.062
5.85	-1.23	0.006	0.032	22.75	4.95	0.030	0.035
6.50	4.11	0.006	0.075	23.40	7.46	0.030	0.062
7.15	7.46	0.006	0.079	24.05	11.02	0.030	0.062
7.80	6.41	0.006	0.070	24.70	20.33	0.030	0.090
8.45	13.65	0.000	0.097	25.35	28.92	0.030	0.146
9.10	22.74	0.006	0.120	26.00	12.59	0.030	0.062
9.75	30.59	0.006	0.140	26.65	8.71	0.030	0.062
10.40	32.89	0.030	0.145	27.30	4.53	0.030	0.035
11.05	11.02	0.030	0.088	27.95	3.38	0.030	0.035
11.70	7.35	0.030	0.068	28.60	4.53	0.030	0.035
12.35	9.13	0.030	0.096	29.25	2.01	0.030	0.035
13.00	4.84	0.030	0.053	29.90	3.17	0.030	0.035
13.65	0.97	0.030	0.039	30.55	3.90	0.030	0.035
14.30	1.81	0.030	0.041	31.20	4.00	0.030	0.035
14.95	0.44	0.030	0.032	31.85	2.22	0.030	0.035
15.60	0.55	0.030	0.032	32.50	4.53	0.030	0.035
16.25	0.44	0.030	0.031	33.15	3.27	0.030	0.035
16.90	0.44	0.030	0.030	33.80	4.00	0.030	0.035

Table A1. Concentrations of Mn, U, and Pb in side canyon porewater, continued

depth	Mn	U	Pb
Navajo Canyon			
17.55	0.49	0.000	0.030
18.20	0.55	0.006	0.029
18.85	0.65	0.030	0.031
19.50	0.76	0.030	0.029
20.15	1.60	0.030	0.032
20.80	0.44	0.006	0.028
21.45	2.75	0.030	0.035
22.10	2.12	0.030	0.032
22.75	0.55	0.030	0.029
23.40	0.34	0.006	0.030
24.05	0.65	0.030	0.029
24.70	0.34	0.006	0.029
25.35	0.76	0.030	0.028
26.00	0.24	0.030	0.026
26.65	0.55	0.006	0.032

Table A2. Concentrations (in μM) of lead (Pb) and arsenic (As) measured during January 2007 in Farley Canyon and White Canyon, Lake Powell; depth (in cm) of 0 is the sediment-water interface

depth	Pb	As	depth	Pb	As
White Canyon, probe A			*Farley Canyon, probe A*		
-11.08	0.029	0.559	-13.24	0.014	0.262
-10.39	0.031	0.211	-12.55	0.013	0.219
-9.70	0.029	0.190	-12.55	0.009	0.237
-9.01	0.015	0.212	-11.86	0.016	0.211
-9.01	0.015	0.225	-11.17	0.022	0.193
-7.63	0.014	0.194	-10.48	0.014	0.171
-7.63	0.011	0.215	-10.48	0.004	0.000
-6.94	0.022	0.188	-9.79	0.014	0.235
-6.25	0.022	0.189	-9.79	-0.015	0.202
-5.56	0.023	0.174	-9.10	0.015	0.230
-4.87	0.023	0.192	-7.72	0.015	0.323
-4.18	0.025	0.197	-6.34	0.012	0.215
-3.49	0.029	0.220	-6.34	0.013	0.208
-2.80	0.028	0.194	-4.96	0.018	0.208
-2.11	0.030	0.214	-4.27	0.015	0.158
-1.42	0.073	0.207	-3.58	-0.007	0.128
-0.73	0.021	0.271	-2.89	0.018	0.198
-0.73	0.000	0.261	-1.51	0.016	0.172
-0.04	0.028	0.205	-0.13	0.017	0.209
0.65	0.035	0.188	1.25	0.018	0.202
1.34	0.024	0.228	1.94	0.016	0.195
2.03	0.026	0.243	2.63	0.017	0.211
2.72	0.025	0.222	3.32	0.021	0.227
4.10	0.025	0.237	4.01	0.017	0.197
4.79	0.018	0.237	4.70	0.053	0.193
4.79	-0.008	0.218	6.08	0.019	0.240
5.48	0.035	0.219	6.77	0.018	0.247
6.17	0.033	0.000	7.46	0.020	0.230
6.86	0.027	0.184	8.15	0.009	0.220
8.24	0.038	0.164	9.53	0.016	0.288
8.93	0.035	0.000	10.22	0.014	0.228
9.62	-0.001	0.172	10.91	0.023	0.244
10.31	0.025	0.209	12.98	0.016	0.237
11.00	0.015	0.246	13.67	0.012	0.245

Table A2. Concentrations lead and arsenic in side canyon porewater, continued

depth	Pb	As	depth	Pb	As
White Canyon, probe A, continued			*Farley Canyon, probe A, continued*		
11.00	0.012	0.275	14.36	-0.012	0.163
12.38	0.023	0.272	15.05	0.017	0.240
13.07	0.048	0.259	15.74	0.013	0.240
13.76	0.045	0.289	16.43	0.019	0.233
14.45	0.034	0.167	17.12	0.012	0.237
15.14	0.022	0.242	19.19	0.019	0.236
15.83	0.026	0.247	20.57	0.017	0.263
17.90	0.016	0.260	21.95	0.020	0.238
18.59	0.023	0.294	22.64	0.023	0.224
19.28	0.019	0.280	24.02	0.019	0.244
19.97	0.022	0.259	24.71	0.020	0.264
21.35	0.028	0.262	25.40	0.015	0.220
Farley Canyon, probe B			26.09	0.022	0.250
-1.15	0.085	0.212	26.78	0.017	0.228
-1.15	0.081	0.210	28.85	0.014	0.255
-0.47	0.018	0.186	30.23	0.013	0.207
0.22	0.024	0.190	30.92	0.019	0.214
0.91	0.019	0.119	31.61	0.020	0.275
0.91	0.019	0.121	32.99	0.018	0.219
1.59	0.022	0.152	*Farley Canyon, probe C*		
2.28	0.020	0.207	-1.15	0.042	0.227
3.65	0.017	0.203	-0.47	0.032	0.198
5.02	0.022	0.191	0.22	0.033	0.232
5.70	0.017	0.185	0.91	0.062	0.212
5.70	0.017	0.218	1.59	0.033	0.237
6.39	0.017	0.191	1.59	0.032	0.228
7.76	0.019	0.219	2.28	0.017	0.205
8.44	0.015	0.165	2.96	0.037	0.154
9.13	0.019	0.208	3.65	0.030	0.201
9.81	0.015	0.231	5.02	0.020	0.225
9.81	-0.011	0.230	5.02	0.020	0.223
10.50	0.016	0.195	5.70	0.027	0.208
11.18	0.021	0.230	6.39	0.030	0.230
11.87	0.024	0.191	6.39	0.011	0.198
12.55	0.012	0.218	7.07	0.026	0.188
13.24	0.017	0.215	7.76	0.027	0.166

Table A2. Concentrations lead and arsenic in side canyon porewater, continued

depth	Pb	As	depth	Pb	As
Farley Canyon, probe B, continued			*Farley Canyon, probe C, continued*		
13.92	0.026	0.253	8.44	0.037	0.213
14.61	0.025	0.180	9.81	0.030	
15.29	0.020	0.257	10.50	0.024	0.154
15.98	0.020	0.221	11.18	0.025	0.237
16.66	0.014	0.236	11.87	0.011	0.201
16.66	-0.010	0.238	12.55	0.026	
17.35	0.012	0.220	13.92	3.173	
18.03	0.020	0.179	14.61	0.018	0.221
18.72	0.025	0.000	15.29	0.021	0.139
19.40	0.013	0.210	15.98	0.015	0.207
20.09	0.013	0.226	15.98	0.013	0.191
20.77	0.020	0.000	16.66	0.015	0.235
21.46	0.015	0.227	17.35	0.014	0.221
22.14	0.015	0.198	18.03	0.012	0.242
22.83	0.012	0.202	18.72	0.127	0.215
23.51	0.014	0.208	19.40	0.015	0.212
24.20	0.012	0.232	20.09	0.017	0.238
24.88	0.017	0.237	20.77	0.090	0.198
25.57	0.021	0.250	21.46	0.017	0.201
26.25	0.010	0.200	22.14	0.021	0.218
26.94	0.015	0.181	22.83	0.017	0.209
27.62	0.016	0.214	23.51	0.016	0.207
28.31	0.018	0.142	24.20	0.018	0.191
28.99	0.013	0.211	24.88	0.017	0.216
30.36	0.021	0.155	25.57	0.017	0.133
31.05	0.023	0.223	26.25	0.017	0.334
31.73	0.015	0.232	26.94	0.017	0.215
32.42	0.012	0.239	27.62	0.024	0.243
32.42	0.011	0.237	28.31	0.021	0.185
33.10	0.019	0.275	28.99	0.018	0.259
33.79	0.070	0.395	29.68	0.015	0.197
			30.36	0.016	0.250
			31.05	0.016	0.174
			31.05	0.016	0.195
			31.73	0.009	0.229
			31.73	0.010	0.277
			32.42	0.017	0.261
			33.10	0.016	0.226